

Constrained variational quantum eigensolver: Quantum computer search engine in the Fock space

Ilya G. Ryabinkin

*Department of Physical and Environmental Sciences,
University of Toronto Scarborough, Toronto, Ontario M1C 1A4, Canada and
Chemical Physics Theory Group, Department of Chemistry,
University of Toronto, Toronto, Ontario M5S 3H6, Canada*

Scott N. Genin

OTI Lumionics Inc., 100 College St. #351, Toronto, Ontario M5G 1L5, Canada

Artur F. Izmaylov

*Department of Physical and Environmental Sciences,
University of Toronto Scarborough, Toronto, Ontario M1C 1A4, Canada and
Chemical Physics Theory Group, Department of Chemistry,
University of Toronto, Toronto, Ontario M5S 3H6, Canada**

(Dated: August 14, 2024)

Variational quantum eigensolver (VQE) is an efficient computational method promising chemical accuracy in electronic structure calculations on a universal-gate quantum computer. However, such a simple task as computing the electronic energy of a hydrogen molecular cation, H_2^+ , is not possible for a general VQE protocol because the calculation will invariably collapse to a lower energy of the corresponding neutral form, H_2 . The origin of the problem is that VQE effectively performs an unconstrained energy optimization in the *Fock* space of the original electronic problem. We show how this can be avoided by introducing necessary constraints directing VQE to the electronic state of interest. The proposed constrained VQE can find an electronic state with a certain number of electrons, spin, or any other property. The new algorithm does not require any additional *quantum* resources. We demonstrate performance of the constrained VQE by simulating various states of H_2 and H_2O on Rigetti Computing Inc’s 19Q-Acorn quantum processor.

Quantum chemistry seeks the exact solution of the electronic Schrödinger equation,¹

$$\hat{H}_e |\Psi_i(\mathbf{R})\rangle = E_i(\mathbf{R}) |\Psi_i(\mathbf{R})\rangle, \quad (1)$$

where \hat{H}_e is the electronic Hamiltonian of a molecule with a fixed nuclear configuration \mathbf{R} , $E_i(\mathbf{R})$ are its eigenvalues, also known as potential energy surfaces (PESs), and $|\Psi_i(\mathbf{R})\rangle$ are the corresponding electronic wavefunctions. Even though this is only the electronic part of the total molecular quantum problem, it determines systems’ properties crucial for designing new materials^{2,3} and pharmaceutical compounds.⁴ The main computational difficulty of tackling this problem is the exponential growth of complexity with the number of interacting particles (*i.e.* electrons). This exponential scaling makes it infeasible to obtain high accuracy for large systems (*e.g.* materials and proteins) on a classical computer. Various approximations compromising the accuracy become necessary.^{1,5}

On the other hand, there is a hope to overcome the exponential scaling by engaging a universal quantum computer.⁶ One of the main practical difficulties remains maintaining large enough number of qubits in a coherent superposition state entangling several particles. Another issue is related to reformulating the electronic structure problem for the quantum computer. The earliest proposal was the quantum phase estimation algorithm,^{7–9} which was quite successful in terms of accuracy but placed strong requirements on quantum hardware to maintain

coherence for a long time. As an alternative with reduced coherency requirements, the variational quantum eigensolver (VQE) has been suggested.^{10–12} Note though that a unitary coupled cluster type of ansatz for the wavefunction used in VQE is *not* rigorously equivalent to the exact solution of the electronic structure problem but rather gives numerical results of chemical accuracy and is exponentially hard for a classical computer.

Recent experimental work by Kandala *et al.*¹³ demonstrated successful quantum simulations by means of the tailored VQE ansatz for PESs of few selected small molecules, H_2 , LiH , and BeH_2 . Despite the impressive results, there were still visible imperfections, “kinks”, in the simulated PESs whose origins were not clear. The authors attributed them to the limited accuracy of simulations and claimed that they could be removed by increasing resource requirements. Yet, it is still desirable to disentangle the difficulties related to experimental realization from a possible incompleteness of the employed formalism. One of the main goals of quantum chemistry is to produce smooth PESs that can be used further in modeling chemical dynamics. Therefore, having kinks is a significant drawback that cannot be left unresolved.

Another problem that has not yet been discussed is how to apply quantum computing in its practical VQE form to obtain information about electronic states with different numbers of electrons (*e.g.* cations and anions) or different spin (*e.g.* singlets, triplets, *etc.*). Turns out that

the key to understanding both problems, eliminating PES kinks and obtaining PESs for different charge and spin electronic states, is the first step in the formulation of the electronic structure problem for quantum computing. To encode the electronic Hamiltonian using qubits one needs to start not with the Hilbert space formulation (1) but rather with the so-called second-quantized formulation of the Hamiltonian, which operates in the Fock space. The Fock space for a particular molecule combines the Hilbert spaces of all molecular forms with all possible number of electrons. This leads to an interesting problem, namely: for molecule A there is only *one* Hamiltonian, whose eigenvalues are electronic energies of A, A^\pm , $A^{2\pm}$, *etc.* Since the electronic energy of a cation is *always* higher than that for a neutral—otherwise a molecule would be autoionizing—it becomes an *excited* state in the full spectrum. Any variational method aimed at *minimizing* the energy will converge to the state of a neutral A, leaving A^+ inaccessible. Even worse, for any molecule with a positive electron affinity the lowest-energy solution is an *anion* rather than the neutral form. A similar situation is with the total electron spin, when the spin multiplicity of the lowest energy state could be different from the one that is of interest.

We will show that in its current form, VQE leads to kinks in PESs due to variational instabilities that cause switches between electronic states of different symmetries within the Fock space. These issues also lead to the inability of current simulation protocols to compute PESs of molecular cations. A particularly simple example of this problem is H_2^+ , which is exactly solvable problem that dates back to the early days of quantum mechanics.^{14,15} We resolve all these issues by introducing the constrained modification of the VQE, which is indispensable for quantum chemistry applications.

I. RESULTS

A. Operators in the Fock and qubit spaces

Formulation of the electronic structure problem for a quantum computer starts from the electronic Hamiltonian \hat{H}_e in the second-quantized form

$$\hat{H}_e = \sum_{ij}^{N_b} h_{ij} \hat{a}_i^\dagger \hat{a}_j + \frac{1}{2} \sum_{ijkl}^{N_b} g_{ijkl} \hat{a}_i^\dagger \hat{a}_k^\dagger \hat{a}_l \hat{a}_j, \quad (2)$$

where \hat{a}_i^\dagger and \hat{a}_i are fermionic creation and annihilation operators corresponding to a one-electron state ϕ_i within an N_b one-electron basis set.¹⁶ The coefficients, h_{ij} and g_{ijkl} , are one- and two-electron integrals, respectively. N_b determines a computational cost of solving the electronic Schrödinger equation because computational expenses grow exponentially with N_b if no approximations are made.

A Hamiltonian of a free molecule in the absence of an external electromagnetic field forms a set of commuting

operators with the electron number operator, \hat{N} , the z -projection of the total molecular spin, \hat{S}_z , and the square of the total spin, \hat{S}^2 . (The last two should not be confused with corresponding qubit operators.) All these operators have the second-quantized forms that can be found in Ref. 16.

Quantum computers employ two-level systems (“qubits”) as the computational basis. Qubits can be thought of as spin-1/2 particles, although real quantum computers may not use genuine spins.^{10,13} The fermionic Hamiltonian (2) is translated from fermionic to qubit representation by one of the fermion-to-qubit mappings, the Jordan–Wigner (JW) or more recent and resource-efficient the Bravy–Kitaev (BK) transformation.^{17,18} After the JW or BK transformations all operators become operators in the qubit space, for instance, \hat{H}_e assumes the form

$$\hat{H} = \sum_I C_I \hat{T}_I, \quad (3)$$

where C_I coefficients are functions of one- and two-electron integrals, and \hat{T}_I operators are products of several spin operators,

$$\hat{T}_I = \omega_0^{(I)} \cdots \omega_k^{(I)}, \quad 0 \leq k \leq N_b - 1. \quad (4)$$

Each of $\omega_i^{(I)}$ denotes one of the Pauli matrices, x_i , y_i , or z_i operating on the i^{th} fictitious spin-1/2 particle that represents the i^{th} qubit. \hat{H} is an N_b -qubit operator that has a $2^{N_b} \times 2^{N_b}$ matrix representations. Importantly, not only the matrix dimension but also the whole spectrum of the qubit Hamiltonian (3) is identical to its fermionic counterpart (2). Thus, finding the eigenstates of the qubit Hamiltonian (3) is equivalent to the solving the quantum chemistry problem.

As an illustration, we consider the H_2 molecule in the minimal STO-3G basis ($N_b = 4$). The fermionic Hamiltonian of this system describes $2^{N_b} = 16$ electronic states. Presence of states of different spin and number of electrons does not pose a difficulty in ordinary quantum chemistry on a classical computer because the electronic Hamiltonian is projected onto a Hilbert subspace corresponding to the electronic state of interest. This projection is done via use of Slater determinants. They implicitly fix the number of particles $N = \langle \hat{N} \rangle$, $S_z = \langle \hat{S}_z \rangle$ and even $S^2 = \langle \hat{S}^2 \rangle$ if appropriate combinations (configurations) of Slater determinants are chosen. Figure 1 presents lowest singlet and triplet electronic PESs of the H_2 molecule and the ground state PES of its cation obtained by the full configuration interaction approach.

Using the BK transformation the electronic Hamiltonian in the STO-3G basis is mapped to the same number ($N_b = 4$) of qubits. The resulting Hamiltonian¹⁹ has 15 terms, each of them is a product of Pauli matrices multiplied by a coefficient inferred from one- and two-electron integrals (h_{ij} and g_{ijkl}) at a given interatomic distance

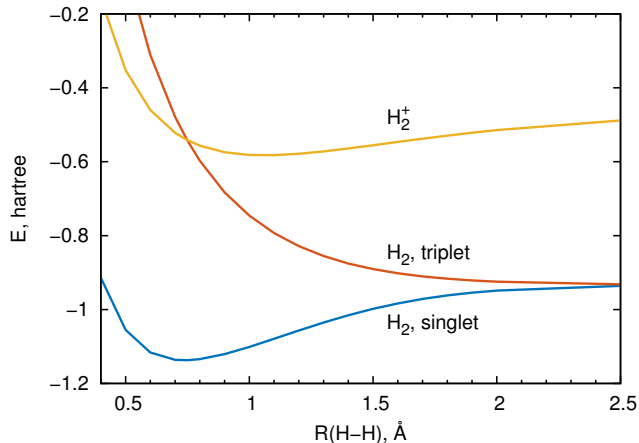


FIG. 1. Two lowest PESs of the H_2 molecule and the ground state PES of the H_2^+ cation obtained using the full configuration interaction method in the STO-3G basis.

R . For example, at $R = 0.75 \text{ \AA}$ we have²⁰

$$\begin{aligned} \hat{H}_{\text{BK}}(R) \Big|_{R=0.75 \text{ \AA}} &= -0.109731 \\ &+ 0.169885 z_0 &+ 0.168212 z_1 \\ &+ 0.169885 z_1 z_0 &+ 0.0454429 x_2 z_1 x_0 \\ &- 0.218863 z_2 &+ 0.0454429 y_2 z_1 y_0 \\ &+ 0.120051 z_2 z_0 &+ 0.165494 z_2 z_1 z_0 \\ &+ 0.173954 z_3 z_1 &+ 0.0454429 z_3 x_2 z_1 x_0 \\ &+ 0.120051 z_3 z_2 z_0 &+ 0.0454429 z_3 y_2 z_1 y_0 \\ &- 0.218863 z_3 z_2 z_1 &+ 0.165494 z_3 z_2 z_1 z_0. \end{aligned} \quad (5)$$

Diagonalization of this Hamiltonian in the $2^{N_b} = 16$ -dimensional qubit space provides the same eigenvalues, but the information about the number of electrons N , or S^2 for corresponding eigenstates is now hidden.

Let us consider the two lowest *exact* PESs of the H_2 molecule that were calculated by full diagonalization of the qubit Hamiltonian $\hat{H}_{\text{BK}}(R)$ for different R (Fig. 2) We track the physical nature of the solutions using properties corresponding to commuting observables: first, we constructed the BK-transformed operators \hat{N} and \hat{S}^2

$$\hat{N}_{\text{BK}} = 2 - (z_0 - z_1 z_0 - z_2 - z_3 z_2 z_1)/2, \quad (6)$$

$$\begin{aligned} \hat{S}_{\text{BK}}^2 &= (6 - 3z_1 + x_2 x_0 - x_2 z_1 x_0 + y_2 y_0 \\ &+ z_2 z_0 - z_2 z_1 z_0 - 3z_3 z_1 - y_2 z_1 y_0 \\ &+ z_3 x_2 x_0 - z_3 x_2 z_1 x_0 + z_3 y_2 y_0 \\ &- z_3 y_2 z_1 y_0 + z_3 z_2 z_0 - z_3 z_2 z_1 z_0)/8 \end{aligned} \quad (7)$$

and then evaluated the mean values of these operators on the calculated exact states. First of all, for $R \leq 0.7 \text{ \AA}$ the first excited state corresponds to the state of H_2^+ , $N = 1$, while for larger R it is a triplet state of the neutral molecule ($N = 2$, $S^2 = 2$). Thus, in the STO-3G basis set the triplet state changes its position in the spectrum as R varies. The cationic ground state is among the excited states and intersects with the triplet H_2 state

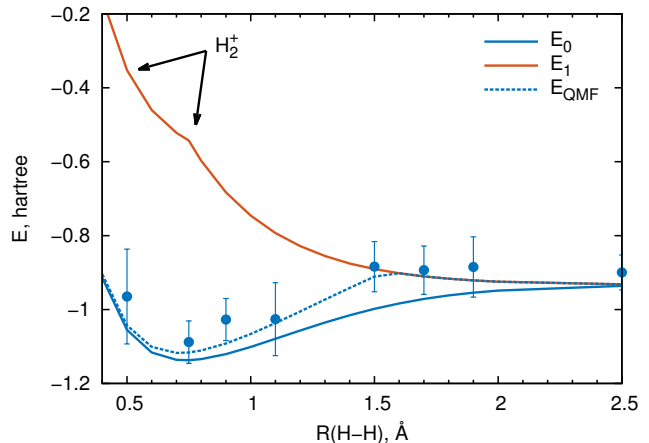


FIG. 2. Two lowest eigenstates of the Hamiltonian $\hat{H}_{\text{BK}}(R)$ (solid lines), and the PES corresponding to the minimum of the QMF functional, Eq. (11) (dashed line). Points with error bars correspond to QMF calculations performed on the Rigetti quantum computer. Error bars show the standard deviation over measured values.

forming a kink due to the energy ordering of the electronic states. Therefore, one of the reasons for appearing kinks in quantum calculations can be intersections of states that originally belonged to different Hilbert spaces of the fermionic problem and brought within the same qubit space by using the Fock-space second-quantized Hamiltonian (2).

B. Variational quantum eigensolver

VQE carries out the optimization of the electronic ground state energy in a two-step procedure. First, the expectation value of the Hamiltonian

$$E(\Omega, \tau) = \langle \Psi(\Omega, \tau) | \hat{H} | \Psi(\Omega, \tau) \rangle \quad (8)$$

was calculated from measurements of individual Pauli terms, \hat{T}_I [Eq. (3)], to obtain corresponding averages $\langle \Psi(\Omega, \tau) | \hat{T}_I | \Psi(\Omega, \tau) \rangle$ and to contract them with C_I at fixed values of wavefunction parameters Ω, τ . Second, the minimization of $E(\Omega, \tau)$ is done on a classical computer

$$E = \min_{\Omega, \tau} E(\Omega, \tau). \quad (9)$$

A typical parametrization of the wavefunction as a N_b -qubit trial state is

$$|\Psi(\Omega, \tau)\rangle = U_{\text{ENT}}(\tau) U_{\text{MF}}(\Omega) |00\dots 0\rangle, \quad (10)$$

where $|00\dots 0\rangle$ is an initialized N_b -qubit state, $U_{\text{MF}}(\Omega)$ is a mean-field rotation of individual qubits and $U_{\text{ENT}}(\tau)$ is an “entangler” that is responsible for post mean-field treatment of electron-electron correlation effects. Entanglers are parametrized as an exponent of multi-qubit anti-hermitian operators that have parametric dependence on components of τ .

For individual qubit rotations in $U_{\text{MF}}(\mathbf{\Omega})$ of Eq. (10), only two out of the three Euler angles change the total energy, and one angle defines a global phase change, which does not affect the energy. A convenient basis for the Hilbert space of individual qubits representing these relations is a basis of spin coherent states,^{21–24} $\{|\Omega\rangle\}$, where $\Omega = (\phi, \theta)$ encodes a position of a qubit orientation on the Bloch sphere (see Methods for more formal definitions). The direct product of individual qubit coherent states forms the N_b -qubit mean-field solution $|\mathbf{\Omega}\rangle = U_{\text{MF}}(\mathbf{\Omega})|00\dots 0\rangle$. The optimal values of $\mathbf{\Omega}$ can be obtained using the variational principle,²⁴ if E_0 is the ground state energy for the Hamiltonian in Eq. (3) then $E_0 \leq \langle \mathbf{\Omega} | \hat{H} | \mathbf{\Omega} \rangle = E_{\text{QMF}}(\mathbf{\Omega})$. Therefore, $\langle \mathbf{\Omega} | \hat{H} | \mathbf{\Omega} \rangle$ defines the *qubit mean-field energy functional*,

$$E_{\text{QMF}}(\mathbf{\Omega}) = \sum_I C_I F_I(\mathbf{n}_1^{(I)}, \dots, \mathbf{n}_{N_b}^{(I)}), \quad (11)$$

where each F_I is obtained from \hat{T}_I by substitution $\omega_i^{(I)} \rightarrow \mathbf{n}_i^{(I)}$ and operator products of $\omega_i^{(I)}$ are converted to ordinary numerical products. $\mathbf{n}_i^{(I)}$ is a shorthand notation for the $\omega_i^{(I)}$ component of the unit vector on a Bloch sphere: $\mathbf{n} = (\cos \phi \sin \theta, \sin \phi \sin \theta, \cos \theta)$.

The ground-state mean-field solution for H_2 , E_{QMF} (Fig. 2), which behaves like the restricted Hartree–Fock (RHF) curve for small R , has a second type of kinks near $R \approx 1.6 \text{ \AA}$. This kink is due to switching of a mean-field minimum from a singlet ($S^2 = 0$) to a triplet ($S^2 = 2$) solution.

To expose the second type of kinks in quantum computing for PESs in their most vivid form we avoided using entanglers. Generally, entanglers are supposed to bring the mean-field solution closer to the exact one. The later is smooth in this case (Fig. 2), and therefore, if the entanglers fully accomplished the task there would be no kink. However, in practical calculations there is no general prescription how to choose the entangler that rigorously guarantees convergence to the exact answer. Thus, any approximate entangler can make kinks originating in mean-field solutions less pronounced but still existent.

C. Constrained Variational Quantum Eigensolver

To modify the variational procedure to include information about N and S^2 of the target state we use the *constrained optimization*. A constrained minimization is readily applicable to VQE by adding a penalty functional

$$\mathcal{E}(\mathbf{\Omega}, \boldsymbol{\tau}, \boldsymbol{\mu}) = \langle \Psi(\mathbf{\Omega}, \boldsymbol{\tau}) | \hat{H} | \Psi(\mathbf{\Omega}, \boldsymbol{\tau}) \rangle + \sum_i \mu_i \left[\langle \Psi(\mathbf{\Omega}, \boldsymbol{\tau}) | \hat{C}_i | \Psi(\mathbf{\Omega}, \boldsymbol{\tau}) \rangle - C_i \right]^2, \quad (12)$$

where \hat{C}_i are constraining operators (*e.g.* \hat{N} , \hat{S}^2 , *etc.*), C_i are their desired mean values, and μ_i are big but fixed numbers.²⁵ Comparing operators in Eqs. (5) and (6)

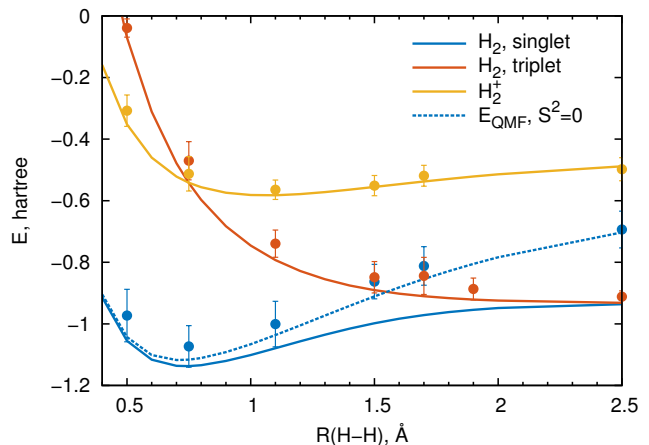


FIG. 3. Three constrained mean-field PESs for lowest singlet ($S^2 = 0$) and triplet ($S^2 = 2$) electronic states of H_2 and the ground electronic state of H_2^+ ($N = 1$). The exact PESs for all but the singlet H_2 state coincide with the constraint mean-field solutions. Points with error bars correspond to constrained QMF calculations performed on the Rigetti quantum computer. Error bars show the standard deviation over measured values.

one can see that they share the same Pauli terms, which means that the value $\langle \Psi(\mathbf{\Omega}, \boldsymbol{\tau}) | \hat{C}_i | \Psi(\mathbf{\Omega}, \boldsymbol{\tau}) \rangle$ can be formed reusing values of $\langle \Psi(\mathbf{\Omega}, \boldsymbol{\tau}) | \hat{T}_I | \Psi(\mathbf{\Omega}, \boldsymbol{\tau}) \rangle$ at zero additional cost.

To obtain lowest energy mean-field solutions of neutral H_2 with well-defined electron spin we minimize the following functional

$$\mathcal{E}_S(\mathbf{\Omega}, \mu) = E_{\text{QMF}}(\mathbf{\Omega}) + \mu \left[\langle \mathbf{\Omega} | \hat{S}_{\text{BK}}^2 | \mathbf{\Omega} \rangle - S^2 \right]^2, \quad (13)$$

where S^2 is either 0 (singlet) or 2 (triplet). The PESs of such constrained minimizations do not exhibit any kinks and retain their target spin values at all R (Fig. 3). The constrained mean-field singlet PES demonstrates the same asymptotic behavior as the RHF curve by going to the incorrect dissociation limit that is exactly in between purely covalent $\text{H} \cdot + \text{H} \cdot$ and ionic $\text{H}^+ + \text{H}^-$ solutions. To correct for this behavior requires an addition of an entangler. On the other hand, the triplet mean-field counterpart reproduces the exact triplet PES because there is no electron-electron correlation for the triplet state in this minimal basis setup.

Similarly, the constrained minimization of the functional

$$\mathcal{E}_N(\mathbf{\Omega}, \mu) = E_{\text{QMF}}(\mathbf{\Omega}) + \mu \left[\langle \mathbf{\Omega} | \hat{N}_{\text{BK}} | \mathbf{\Omega} \rangle - 1 \right]^2 \quad (14)$$

that imposes the $N = 1$ constraint has been employed to extract the lowest PES of H_2^+ (Fig. 3). The resulting curve is smooth and coincides with the exact H_2^+ PES due to the absence of electron-electron correlation.

The constrained methodology can be easily extended to larger systems where constraints become especially useful due to increasing density of electronic states. As an example, we consider the ground singlet state of the

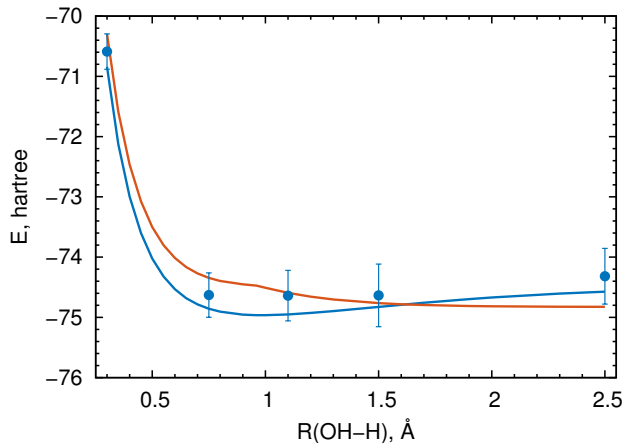


FIG. 4. Restricted Hartree-Fock PESs for the lowest singlet (blue line) and triplet (red line) electronic state of H_2O obtained on a classical computer. Points with error bars correspond to the constrained QMF calculations for the lowest singlet state performed on the Rigetti quantum computer. Error bars show the standard deviation over measured values.

water molecule in the STO-3G basis. Figure 4 shows its PES obtained by changing a single OH-bond length from the symmetric equilibrium configuration with $R(\text{OH})=0.9605\text{\AA}$ and $\angle\text{HOH}=104.95^\circ$. Here, we used both spin ($S=0$) and number of electrons ($N_e=10$) constraints to obtain the mean-field solution. The spin constraint is invaluable for avoiding convergence to the closely spaced triplet solution (Fig. 4).

Another advantage of using the constraints in quantum computing is their capacity to reduce the noise in the measurement process.²⁶ Generally, there are two sources of uncertainty when the Hamiltonian components are measured in the quantum computer: 1) the wavefunction encoded in qubits is not an eigenfunction of a particular Pauli word (T_I) and hence there is an intrinsic quantum uncertainty for the T_I measurement, 2) uncontrolled interactions of qubits with their environment that introduce all sorts of noise unrelated to the ideal, quantum uncertainty. A typical measurement on a quantum computer produces an eigenstate of a measured Pauli word, T_I . We found that re-weighting results of the measurement based on overlaps of a collapsed wavefunction with eigenfunctions of the property operators (*e.g.* \hat{N} and \hat{S}^2) with target eigenvalues (fixed charge and spin) strongly reduces the noise coming from the second source, and does not alter the statistics originating from the truly quantum uncertainty. Our constraint based post-processing scheme is detailed in the Methods section.

D. Discussion

We have proposed a simple constrained VQE approach that is *indispensable* if one seeks a solution of a quantum chemistry problem for an electronic state with a well-defined electronic spin, charge, or any other property

of interest. The corresponding procedure requires minimal modification of the current VQE protocol and incurs virtually no additional *quantum* costs. Using the constrained VQE not only allows one to target specific states but also removes kinks in PESs arising due to numerical instabilities associated with the root switching.

In the current study only the electron number and the total spin operators have been used for imposing constraints. The z -projection of the total electron spin (\hat{S}_z) has not been constrained, although it is another symmetry that one can use. We found that restriction of S_z was not giving any improvements in the considered cases.

Moreover, the operators of conserved quantities can be used to post-process the results of measurements done on the quantum computer to reduce the noise due to qubit interactions with the environment. This post-processing does not affect the statistics of the true quantum distribution arising from the ideal projective measurement.

II. METHODS

A. Spin coherent states

A spin coherent state, also known as a ‘‘Bloch state’’, for a single particle with spin J ($J \geq 0$ is integer or half-integer) is defined by the action of an appropriately scaled exponent of the lowering operator \hat{S}_- on the normalized eigenfunction of \hat{S}_z operator, $\hat{S}_z |JM\rangle = M |JM\rangle$, with maximal projection $M = J$:²⁴

$$\begin{aligned} |\Omega\rangle &= \cos^{2J} \left(\frac{\theta}{2} \right) \exp \left[\tan \left(\frac{\theta}{2} \right) e^{i\phi} \hat{S}_- \right] |JJ\rangle \\ &= \sum_{M=-J}^J \binom{2J}{M+J}^{1/2} \\ &\quad \times \cos^{J+M} \left(\frac{\theta}{2} \right) \sin^{J-M} \left(\frac{\theta}{2} \right) e^{i(J-M)\phi} |JM\rangle, \end{aligned} \quad (15)$$

where the $|JM\rangle$ states are normalized as

$$|JM\rangle = \binom{2J}{M+J}^{1/2} [(J-M)!]^{-1} S_-^{J-M} |JJ\rangle. \quad (16)$$

$\{|\Omega\rangle\}$ constitute an overcomplete non-orthogonal set of states on a unit Bloch sphere parametrized by spherical angles $\Omega = (\phi, \theta)$, $0 \leq \phi < 2\pi$, $0 \leq \theta \leq \pi$.

B. Classical minimization

Constrained [Eqs. (13) and (14)] and unconstrained [Eq. (11)] minimizations on a classical computer were done using the sequential quadratic programming (SQP) algorithm as implemented by the `fmincon` routine of the

MATLAB²⁷ software. All mean-field solutions were obtained by minimizing the corresponding energy functions with respect to all $4 \times 2 = 8$ Bloch angles.

C. Quantum computer simulation details

We performed the simulations on the Rigetti 19Q-Acorn quantum processor unit (QPU)²⁸ using pyQuil and Forest API.²⁹ Our wavefunction ansatz was obtained performing RZ and RX gate operations on individual qubits. This corresponds to mean-field rotations, *i.e.* without qubit entanglement. Qubits were selected based on ensuring the one gate fidelity of the qubits were greater than 0.99.

After the BK transformation, terms of the resulting Hamiltonian that form a mutually commutative set of operators are grouped together to perform a measurement on all of them at the same time. Since all the operators within a commutative set share eigenfunctions this procedure reduces the spread of measurement results due to general non-commutativity of the BK Hamiltonian and its terms.

The expectation value of each commutative group was obtained by averaging over 1000 and 10000 measurements for H₂ and H₂O, respectively. A post-processing procedure removing results with incorrect electron numbers and spin evaluated for each read was used for these measurements. It is shown below that this post-processing only removes results that appear due to experimental noise and does not alter quantum distributions of measurements. Upon assembling the expectation value of the total Hamiltonian from the expectation values of commutative groups, this procedure was repeated 20 (4) times for H₂ (H₂O) to obtain representative statistics for the Hamiltonian expectation values. Averages and standard deviations calculated over these 20 (4) Hamiltonian expectation values are reported as the final averages and standard deviations obtained on the QPU. Since our time was limited on the Rigetti system, we were not able to perform a more in-depth sampling procedure. All four experiments were performed in 24 hours over the course of 5 sessions.

The classical optimization step for the VQE, we implemented the Nelder-Mead (NM) algorithm.³⁰ Methods such as conjugate gradient descent were tried, but the NM algorithm demonstrated more robustness to the noise that was generated by errors.

D. Post-processing procedure

a. Description of the procedure. For the illustration purpose, let us assume that our Hamiltonian has two non-commuting parts, $\hat{H} = \hat{A} + \hat{B}$, $[\hat{A}, \hat{B}] \neq 0$ (*e.g.* \hat{A} and \hat{B} are two non-commuting Pauli words). Estimating the average of \hat{H} on a wavefunction $|\Psi\rangle$ is done by adding the averages from non-commuting parts, $\langle \Psi | \hat{H} | \Psi \rangle = \langle \Psi | \hat{A} | \Psi \rangle + \langle \Psi | \hat{B} | \Psi \rangle$. The averages for both

parts are computed by doing repetitive measurements, but these measurements collapse $|\Psi\rangle$ to different eigenfunctions because 1) \hat{A} and \hat{B} do not share eigenfunctions, and 2) $|\Psi\rangle$ is not generally an eigenfunction of \hat{A} or \hat{B} . If we denote the eigenfunctions and eigenvalues of \hat{A} (\hat{B}) as $|f_n\rangle$ ($|g_n\rangle$) and a_n (b_n), respectively, then the Hamiltonian average is

$$\langle \Psi | \hat{H} | \Psi \rangle = \sum_n a_n |\langle \Psi | f_n \rangle|^2 + b_n |\langle \Psi | g_n \rangle|^2. \quad (17)$$

The probabilities $|\langle \Psi | f_n \rangle|^2$ and $|\langle \Psi | g_n \rangle|^2$ are not measured but instead emerge as a result of collecting results of individual measurements of \hat{A} and \hat{B} . The post-processing procedure simply removes the eigenvalues a_n and b_n if corresponding eigenfunctions $|f_n\rangle$ and $|g_n\rangle$, available as readouts of QPU, violate the correct number of electrons (or any other known good quantum number).

b. Invariance of the quantum average to the procedure. The post-processing procedure based on the electron number operator is equivalent to introducing a projector $\hat{P}_N = |N\rangle \langle N|$ to the eigen-subspace corresponding to the correct number of electrons, $\hat{N} |N\rangle = N |N\rangle$,

$$\langle \Psi | \hat{P}_N \hat{H} \hat{P}_N | \Psi \rangle = \sum_n a_n |\langle \Psi | \hat{P}_N | f_n \rangle|^2 + b_n |\langle \Psi | \hat{P}_N | g_n \rangle|^2. \quad (18)$$

Indeed, eigenvalues associated with $|\langle \Psi | \hat{P}_N | f_n \rangle|^2$ and $|\langle \Psi | \hat{P}_N | g_n \rangle|^2$ will not contribute if corresponding eigenfunctions are orthogonal to the N -subspace: $\hat{P}_N |f_n\rangle = 0$ and $\hat{P}_N |g_n\rangle = 0$. On the other hand, assuming that $|\Psi\rangle$ is within the N -subspace, $\langle \Psi | \hat{P}_N = \langle \Psi |$, it is straightforward to see that $\langle \Psi | \hat{P}_N \hat{H} \hat{P}_N | \Psi \rangle = \langle \Psi | \hat{H} | \Psi \rangle$, and hence, the Hamiltonian expectation values are not affected by the post-processing procedure.

c. Noise reduction. To understand how the post-processing reduces the noise related to uncontrolled qubit interactions with its environment, it is convenient to employ the density matrix formalism. Let us denote the ideal pure-state density as $\rho_0 = |\Psi_0\rangle \langle \Psi_0|$, while the real mixed-state density, appearing due to spurious interactions, is $\rho = \sum_{i=0} \omega_i |\Psi_i\rangle \langle \Psi_i|$. Some components associated with the noise ($\{|\Psi_i\rangle\}_{i \neq 0}$) violate the correct value for the number operator, and therefore, $\hat{P}_N |\Psi_i\rangle = 0$, we will refer to the associated part of the density as reducible, ρ_R , while the rest of ρ will be referred as irreducible, $\rho_I = \hat{P}_N \rho \hat{P}_N$. Clearly, substituting the Hamiltonian average with ρ , $\bar{E} = \text{Tr}[\rho \hat{H}] / \text{Tr}[\rho]$, by that with ρ_I , $\bar{E}_I = \text{Tr}[\rho_I \hat{H}] / \text{Tr}[\rho_I]$ makes results more accurate because of the noise reduction. By repeating the arguments shown for the pure state consideration, it is straightforward to show that the post-processing procedure removes the reducible part of the density in the Hamiltonian average, and hence it produces a more accurate average.

E. Acknowledgements

The authors thank P. Brumer, M. Mosca, and V. Gheorghiu for stimulating discussions. The authors are grateful to the support that Will Zeng, Nick Rubin, and Ryan Karle provided in terms of discussion of applying the theory onto their hardware and for access to the 19Q-Acorn

Quantum computer. OTI Lumionics Inc. would like to acknowledge the support of the Creative Destruction Lab provided in facilitating the interbusiness collaborations between OTI Lumionics Inc. and Rigetti Computing Inc. A.F.I. acknowledges financial support from Natural Sciences and Engineering Research Council of Canada through the Engage grant.

-
- * artur.izmaylov@utoronto.ca
- ¹ T. Helgaker, P. Jorgensen, and J. Olsen, *Molecular Electronic-structure Theory* (Wiley, 2000).
 - ² R. M. Martin and R. M. Martin, *Electronic Structure: Basic Theory and Practical Methods* (Cambridge University Press, 2004).
 - ³ R. Prasad, *Electronic Structure of Materials* (Taylor & Francis, 2013).
 - ⁴ K. Roy, *Quantitative Structure-Activity Relationships in Drug Design, Predictive Toxicology, and Risk Assessment* (IGI Global, 2015).
 - ⁵ R. G. Parr and W. Yang, *Density-functional theory of atoms and molecules*, Vol. 16 (Oxford University Press, 1989).
 - ⁶ M. Nielsen and I. Chuang, *Quantum Computation and Quantum Information: 10th Anniversary Edition* (Cambridge University Press, 2010).
 - ⁷ D. S. Abrams and S. Lloyd, *Phys. Rev. Lett.* **79**, 2586 (1997).
 - ⁸ D. S. Abrams and S. Lloyd, *Phys. Rev. Lett.* **83**, 5162 (1999).
 - ⁹ A. Aspuru-Guzik, A. D. Dutoi, P. J. Love, and M. Head-Gordon, *Science* **309**, 1704 (2005).
 - ¹⁰ A. Peruzzo, J. McClean, P. Shadbolt, M.-H. Yung, X.-Q. Zhou, P. J. Love, A. Aspuru-Guzik, and J. L. O’Brien, *Nat. Commun.* **5**, 4213 (2014).
 - ¹¹ P. J. J. O’Malley, R. Babbush, I. D. Kivlichan, J. Romero, J. R. McClean, R. Barends, J. Kelly, P. Roushan, A. Tranter, N. Ding, B. Campbell, Y. Chen, Z. Chen, B. Chiaro, A. Dunsworth, A. G. Fowler, E. Jeffrey, E. Lucero, A. Megrant, J. Y. Mutus, M. Neeley, C. Neill, C. Quintana, D. Sank, A. Vainsencher, J. Wenner, T. C. White, P. V. Coveney, P. J. Love, H. Neven, A. Aspuru-Guzik, and J. M. Martinis, *Phys. Rev. X* **6**, 031007 (2016).
 - ¹² J. I. Colless, V. V. Ramasesh, D. Dahlen, M. S. Blok, M. E. Kimchi-Schwartz, J. R. McClean, J. Carter, W. A. de Jong, and I. Siddiqi, *Phys. Rev. X* **8**, 011021 (2018).
 - ¹³ A. Kandala, A. Mezzacapo, K. Temme, M. Takita, M. Brink, J. M. Chow, and J. M. Gambetta, *Nature* **549**, 242 (2017).
 - ¹⁴ A. H. Wilson, *Proc. Royal Soc. A* **118**, 635 (1928).
 - ¹⁵ P. M. Morse and E. C. G. Stueckelberg, *Phys. Rev.* **33**, 932 (1929).
 - ¹⁶ T. Helgaker, P. Jorgensen, and J. Olsen, “Molecular electronic-structure theory,” (Wiley, 2000) Chap. 2, pp. 39–40.
 - ¹⁷ J. T. Seeley, M. J. Richard, and P. J. Love, *J. Chem. Phys.* **137**, 224109 (2012).
 - ¹⁸ A. Tranter, S. Sofia, J. Seeley, M. Kaicher, J. McClean, R. Babbush, P. V. Coveney, F. Mintert, F. Wilhelm, and P. J. Love, *Int. J. Quantum Chem.* **115**, 1431 (2015).
 - ¹⁹ All Hamiltonians are generated using the OpenFermion software.³¹
 - ²⁰ The nuclear-nuclear repulsion energy $1/R = 0.705333$ a.u. is included in this Hamiltonian.
 - ²¹ A. Perelomov, *Generalized Coherent States and Their Applications*, Theoretical and Mathematical Physics (Springer Science & Business Media, 2012).
 - ²² J. M. Radcliffe, *J. Phys. A*, **4**, 313 (1971).
 - ²³ F. T. Arecchi, E. Courtens, R. Gilmore, and H. Thomas, *Phys. Rev. A* **6**, 2211 (1972).
 - ²⁴ E. H. Lieb, *Commun. Math. Phys.* **31**, 327 (1973).
 - ²⁵ J. Nocedal and S. J. Wright, “Numerical optimization,” (Springer New York, 2006) Chap. 17, 2nd ed.
 - ²⁶ N. C. Rubin, R. Babbush, and J. McClean, arXiv.org, 1 (2018), 1801.03524v1.
 - ²⁷ MATLAB, *version 8.6.0.267246 (R2015b)* (The MathWorks Inc., Natick, Massachusetts, 2015).
 - ²⁸ J. S. Otterbach, R. Manenti, N. Alidoust, A. Bestwick, M. Block, B. Bloom, S. Caldwell, N. Didier, E. S. Fried, S. Hong, P. Karalekas, C. B. Osborn, A. Papageorge, E. C. Peterson, G. Prawiroatmodjo, N. Rubin, C. A. Ryan, D. Scarabelli, M. Scheer, E. A. Sete, P. Sivarajah, R. S. Smith, A. Staley, N. Tezak, W. J. Zeng, A. Hudson, B. R. Johnson, M. Reagor, M. P. da Silva, and C. Rigetti, arXiv.org (2017), 1712.05771v1.
 - ²⁹ R. S. Smith, M. J. Curtis, and W. J. Zeng, arXiv.org (2016), 1608.03355v2.
 - ³⁰ J. Nelder and R. Mead, *Comput. J.* **7**, 308 (1965).
 - ³¹ J. R. McClean, I. D. Kivlichan, D. S. Steiger, Y. Cao, E. S. Fried, C. Gidney, T. Häner, V. Havlíček, Z. Jiang, M. Neeley, J. Romero, N. Rubin, N. P. D. Sawaya, K. Setia, S. Sim, W. Sun, K. Sung, and R. Babbush, ArXiv e-prints (2017), arXiv:1710.07629 [quant-ph].